Effect of Furfural Residue Ash (FRA) as Additive on Portland Cement and Magnesium Oxysulfate Cement

Yining Sun,[a,b] Ruize Sun,[a,c] Xin Jia,[a] Ping An,[a] Yujian Liu,[a,c] Jinjie Wu,[a,c] Xingfei Song,[a,c,*] and Guangwen Xu [a,*]

**Corresponding author: songxingfei@126.com*

DOI: 10.15376/biores.19.4.8947-8958

GRAPHICAL ABSTRACT

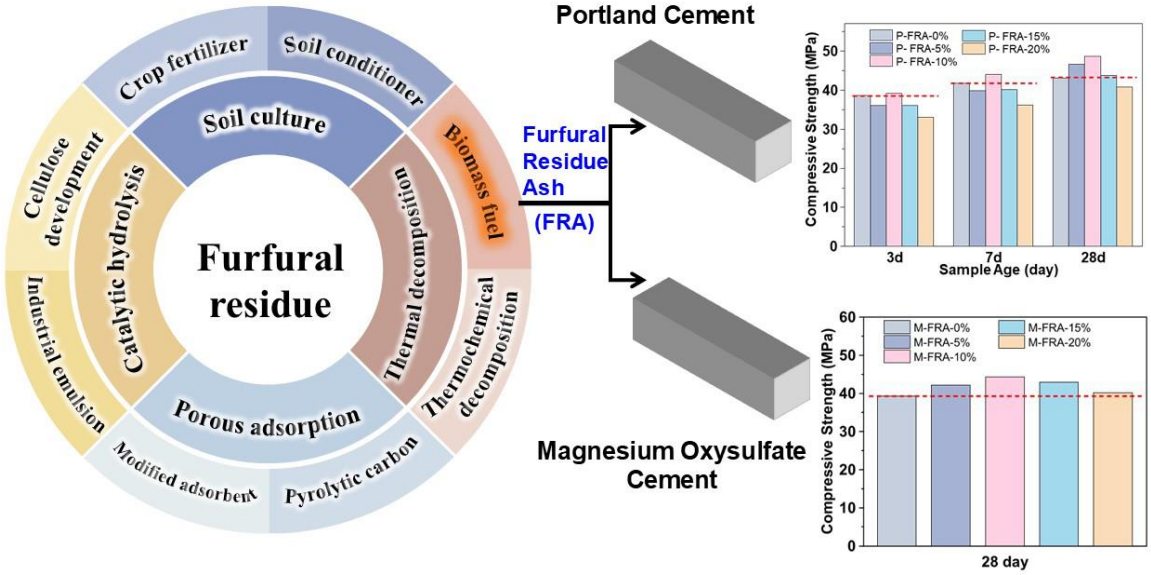

Effect of Furfural Residue Ash (FRA) as Additive on Portland Cement and Magnesium Oxysulfate Cement

Yining Sun,[a,b] Ruize Sun,[a,c] Xin Jia,[a] Ping An,[a] Yujian Liu,[a,c] Jinjie Wu,[a,c] Xingfei Song,[a,c,*] and Guangwen Xu [a,*]

The global production of furfural generates substantial amounts of furfural residue waste annually, which, if not properly managed, can lead to significant environmental pollution. However, the ash produced from the combustion of this biomass waste shows promise as a cement additive, offering an innovative solution for furfural residue management. In this study, ash obtained from the combustion of furfural residue in industrial boilers was used as an additive in both Portland cement and magnesium oxysulfate cement, with concentrations ranging from 5% to 20%. Mortar specimens were then prepared and tested for compressive and flexural strength at 3, 7, and 28 days. The results indicated that at a 10 wt% addition, the formation of cotton-like structures and ettringite needles was most pronounced, resulting in the highest compressive and flexural strengths in the Portland cement specimens. Similarly, in magnesium oxysulfate cement, a 10 wt% ash addition significantly promoted the formation of the 5·1·7 phase, leading to the highest compressive strength. In summary, under appropriate conditions, furfural residue ash can be effectively utilized as a cement additive, contributing to resource recovery and sustainable waste management.

DOI: 10.15376/biores.19.4.8947-8958

Keywords: Furfural residue ash; Portland cement; Magnesium oxysulfate cement; Cement additive

*Contact information: a: Key Laboratory on Resources Chemicals and Materials of Ministry of Education, Shenyang University of Chemical Technology, 11th Street, Shenyang, 110142, PR China; b: School of Chemical Engineering, University of Science and Technology Liaoning, Anshan 114051, China; c: College of Chemical Engineering, Shenyang University of Chemical Technology, 11th Street, Shenyang, 110142, PR China; *Corresponding author: songxingfei@126.com*

INTRODUCTION

Furfural is commonly produced through the dehydration of hemicellulose, specifically pentose sugars derived from agricultural residues like rice hulls, bagasse, and corn cobs (Rachamontree *et al*. 2020). It is one of the top 30 high-value bio-based chemicals (Yemiş and Mazza 2011). The production of one ton of furfural results in the generation of 12 to 15 tons of furfural residue, which is a solid waste with bulky volume (Mao *et al*. 2019). Over 300 kilotons of furfural are produced annually worldwide. Therefore, the estimated annual production of furfural residue is approximately 7 million tons (Inkoua *et al*. 2022).

The composition of furfural residue is complex. The main components are lignin (35 wt%) and cellulose (30 wt%), with a small amount of hemicellulose (5 wt%) (Wang *et al*. 2017). In addition, the residue contains inorganics that were present in the feedstock, the primary catalyst (sulfuric acid) used in furfural production, and other salts (Liu *et al*.

2020). The substantial accumulation of this residue poses a risk of soil, air, and river pollution, contributing to significant environmental challenges (Ranjbari *et al*. 2022).

As shown in Fig. 1, there are basically four ways to make FR into value-added products.

(1) *Soil culture*. Utilizing furfural residue involves two fundamental principles: one involves using its innate acidity to neutralize alkalinity or establish an acidic soil environment, while the other focuses on enhancing soil structure and providing fertilizer for crops.

(2) *Catalytic hydrolysis*. Due to the weak intermolecular forces, furfural residue can easily produce cellulosic ethanol by catalytic hydrolysis (Smit and Huijgen 2017).

(3) *Thermal decomposition*. As a kind of special biomass, furfural residue can be transformed into biochar, bio-oil, and gases (Guo *et al*. 2022) *via* pyrolysis. In addition, the fluffy, porous structure and high carbon content of furfural residue render it feasible for transformation into biochar (Jiang *et al*. 2019).

(4) *Porous adsorption*. FR shows strong absorption capacity on some materials such as methyl blue and methyl violet.

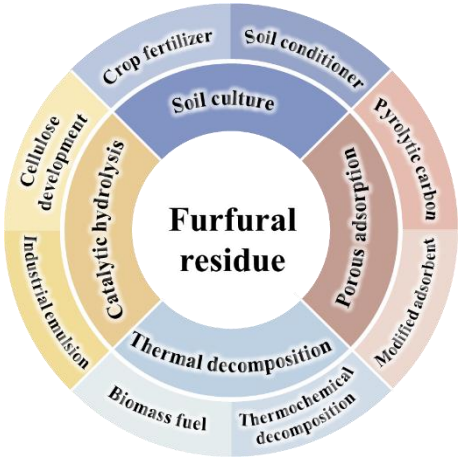

Fig. 1. Four ways to improve FR economic value

Global energy-related CO_2 emission hit a historic peak of 37.4 Gt in 2023 (IEA 2024). Typically, there are five primary emission sectors: energy systems, industrial activities, agriculture, transportation, and buildings. Cement plants are the second-biggest industrial carbon dioxide emitter (He *et al.* 2019). Throughout the cement production process, the thermal synthesis (roasting) of calcium, silicon, and aluminum oxides at high temperatures and the thermal breakdown of carbonates are the main chemical events. Therefore, cement is a typical thermochemical reaction research field (Guo *et al.* 2023; Xu *et al.* 2023). A total of 600 to 900 kg of CO_2 is released throughout each ton of Portland cement clinker processing, which involves converting calcium carbonate into calcium oxide, and during the processing and grinding steps (Favier *et al.* 2018). Strategies including carbon reduction, carbon substitution, and carbon recycling can successfully mitigate carbon emissions from major carbon emitters (Han *et al.* 2023; Song *et al.* 2024). Lowering the clinker amount is one way to reduce CO_2 emissions. Thus, there have been numerous studies on the utilization of various waste materials as substitutes for cement to reduce CO_2 emissions and resolve the waste dumping issue, such as waste paper (Solahuddin and Yahaya 2022), waste rubber (Chou *et al.* 2007), ground granulated blast

furnace slag (Samad *et al.* 2017), biochar from wood (Sirico *et al.* 2021), rich husk ash (Bie *et al.* 2015), and metakaolin (Stonis *et al.* 2013). The utilization of corn cob ash (CCA), which has shown pozzolanic capabilities as a partial replacement for cement, has proven beneficial in some research studies. Endashaw (2022) found that using CCA as filler led to very good resistance to moisture-induced damage. Oriola *et al*. (2023) found that CCA can be used as a partial cement replacement, but the proportion should not be more than 10% replacement considering the compressive strength results. Adesanya and Raheem (2009) found that the CCA did not improve the compressive strength during the initial stages of the concrete's production. Rather, it only functioned as an inert filler. While it can increase compressive strength at a later age (>120 days), compressive strength often decreases with increasing CCA fraction. Oluremi *et al*. (2023) found that the incorporation of CCA decreased the compressive strength of the concrete whereas nano-silica increased the compressive strength. The different research results might be due to different sources such as physical properties of the combustion conditions. Nonetheless, the usual range of the best CCA substitution varies by 5 to 10% depending on the binder's weight.

In this study, the feasibility of using FRA obtained from an industrial boiler as a cement additive was investigated. Initially, the properties of FRA were analyzed using XRD and XRF techniques. Subsequently, silicate cement and magnesium oxysulfate cement mortar specimens were prepared with varying proportions of FRA, and their compressive and flexural strengths were tested at different curing ages (3, 7, and 28 days). Finally, SEM and XRD analyses were conducted to elucidate the reasons for the observed changes in strength. This study offers a methodology for the disposal of FRA, contributing to waste reduction, resource conservation, and carbon dioxide emission mitigation.

EXPERIMENTAL

Materials

The FR used in this research was sourced from Liaoning Quankang Furfural Co., Ltd., located in Chaoyang, China. The results of the proximate and ultimate analyses are presented in Table 1. The FRA was initially collected after combustion in a fluidized bed at temperatures ranging from 900 to 1000 °C, and then sieved to obtain a 325 mesh FRA. The XRF and XRD results are shown in Table 2 and Fig. 2. SiO_2 (39.2%) is a key component of cement, contributing to the formation of calcium silicate hydrate (C-S-H), the primary source of strength during cement hardening. Higher SiO_2 content enhances compressive strength and durability. K_2O (16.1%) acts as a flux to lower the melting temperature of raw materials during cement production, but excess amounts can trigger alkali-silica reaction (ASR), leading to cracks in concrete, necessitating controlled levels. SO_3 (13.9%) regulates cement setting time by forming calcium sulfate (gypsum), preventing rapid setting and ensuring workability.

Table 1. Proximate and Ultimate Analyses of FR

Proximate Analysis (%)			Ultimate Analysis (%)				
A_{ad}	V_{ad}	FC_{ad}	C	H	O*	N	S
7.68	66.4	25.9	47.3	4.7	46.6	0.57	0.90

* Determined by difference

Table 2. XRF Results of FRA

Chemical Composition	FRA (%)	Chemical Composition	FRA (%)	Chemical Composition	FRA (%)
SiO_2	39.2	Cl	2.91	ZrO_2	0.05
K_2O	16.1	P_2O_5	2.47	SrO	0.04
SO_3	13.9	Na_2O	2.47	ZnO	0.03
CaO	8.03	MgO	1.70	Cr_2O_3	0.02
Al_2O_3	7.86	TiO_2	1.02	Rb_2O	0.02
Fe_2O_3	4.14	MnO	0.09		

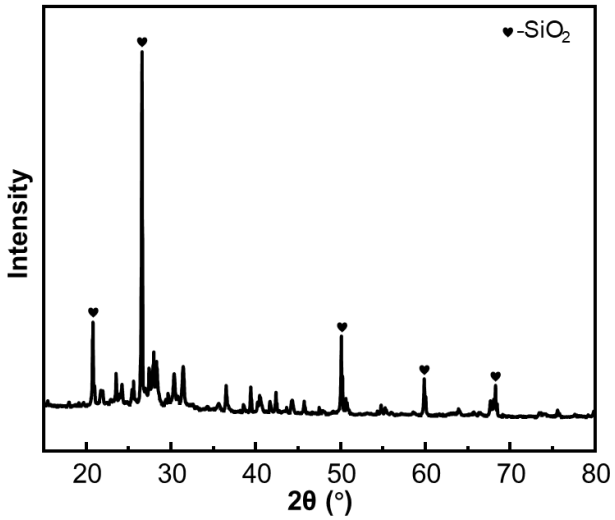

Fig. 2. XRD results of FRA

Preparation of Portland Cement Mortar Specimen

Portland cement mortar paste samples were prepared using a commercial P.O 42.5 Portland cement manufactured by Shenyang Jidong Cement Co., LTD, in accordance with GB 175-2007 standards. Details regarding its chemical composition and several physical properties are listed in Table 3.

Table 3. Mechanical and Physical Properties of Cement

Specific Surface Area (m^2/kg)	Cement Setting Time (min)		SO_3 (%)	MgO (%)	L.O.I (%)	Flexural Strength (MPa)		Compressive Strength (MPa)	
	Initial	Final							
364	175	227	2.05	4.31	2.91	5.9 (3d)	9.0 (28d)	29.2 (3d)	53.6 (28d)

The standard sand was manufactured by Xiamen ISO Standard Sand Co., Ltd, in compliance with GB/T 17671, equivalent to ISO 677 and EN 196-1 standards. The silicon oxide content in standard sand was greater than 98%, and the moisture content was less than 0.2%. The size distribution of aggregates is presented in Table 4.

Table 4. Particle Distribution of Standard Sand

Sieve size (mm)	2.00	1.60	1.00	0.50	0.16	0.08
Cumulative passing (%)	0	7±5	33±5	67±5	87±5	99±1

The control mortar specimen with dimensions of 40×40×160 mm was prepared with a cement-to-standard sand-to-water ratio of 1:3:0.5, following the specifications outlined in China's GB/T 17671-1999 (1999) standard. After 24 h, the specimens were removed from the molds and stored in a cabinet maintained at no less than 90% relative humidity and a temperature of 20±2 °C until testing. To evaluate the impact of different ratios of FRA as a cement additive on the strength of the mortar, samples were prepared with FRA replacing 0% to 20% of the cement by weight, in 5% increments.

As shown in Table 5, different Portland specimen samples are designated with similar names throughout this paper. For instance, P-FRA-0% represents the mortar sample without FRA, whereas P-FRA-5%, P-FRA-10%, P-FRA-15%, and P-FRA-20% denote mortar samples incorporating FRA as a cement additive at 5%, 10%, 15%, and 20% of the cement weight, respectively.

Table 5. Portland Cement Mortar Mixture Proportions

Samples	Replacement (%)	Cement (g)	Standard Sand (g)	FRA (g)	Water (mL)
P-FRA-0%	0	450.0	1350	0	225
P-FRA-5%	5	427.5		22.5	
P-FRA-10%	10	405.0		45.0	
P-FRA-15%	15	382.5		67.5	
P-FRA-20%	20	360		90	

Preparation of Magnesium Oxysulfate Cement Mortar Specimen

The molar ratio of the raw materials for preparing magnesium thioglycolate cement samples was set as n(α-MgO): n($MgSO_4$): n(H_2O) = 8:1:16. The detailed experimental formulations are shown in Table 3. An external admixture method was uniformly used to incorporate citric acid and FRA, with the amounts of admixtures calculated based on the mass percentage of magnesium oxide.

Table 6. Magnesium Oxysulfate Cement Mortar Mixture Proportions

Samples	n(α-MgO) : n($MgSO_4$) : n(H_2O)	Citric Acid (g)	FRA (g)
M-FRA-0%	8:1:16	3.46	0
M-FRA-5%			18.2
M-FRA-10%			36.4
M-FRA-15%			54.6
M-FRA-20%			72.8

Magnesium sulfate heptahydrate was dissolved in warm water with stirring. Based on the mass percentage of magnesium oxide, the required modifiers and FRA were measured and mixed. The pre-weighed magnesium oxide powder was then gradually added and stirred at 800 r/min for 4 min to form a homogeneous cement paste. The paste was poured into 40×40×160 mm molds, vibrated, and leveled. The molds were placed in a chamber at 25 ± 2 °C and 65 ± 5% relative humidity for curing. After curing, the specimens were demolded and further cured until the specified age.

Test Methods

The compressive and flexural strengths of the cement mortar were tested using a computerized, fully automatic cement bending and compression testing machine (DYE-300S, Hebei Chen Xin Testing Machine Make Co., Ltd., Cangzhou, China) in accordance with the JC/T 724-2005 standard (2005). During the tests, the loading rates for compressive and flexural strength were 1600 N/s and 50 N/s, respectively. The experiments were conducted at 3, 7, and 28 days. The reported compressive and flexural strengths are the averages of three and six samples, respectively.

The cement mortar samples were first coated with 10 to 20 nm thick gold films and then examined using a SEM (JSM-IT800, Nihon Electronics, Japan) at an accelerating voltage of 30 kV. The crystal structures of various cement mortar samples were determined by a XRD (Rigaku Ultima IV, Japan) with the following setup parameters: wavelength of 1.5418 Å, voltage of 40 kV, current of 40 mA, and scanning rate of 1°/min.

RESULTS AND DISCUSSION

Strength of Portland cement mortar

The compressive and flexural strength data of FRA blended Portland mortar are shown in Fig. 3. At 3 and 7 days, only compressive strength of P-FRA-10% was higher than that of P-FRA-0% (control sample). Additionally, at 28 days P-FRA-10% and P-FRA-5% samples were 1.08 and 1.13 times higher than P-FRA-0%, respectively. In Fig. 3b at 3 days, it can be seen that only the flexural strengths of P-FRA-0% was the lowest with a value of 3.9 MPa. At 7 days, only the flexural strengths of P-FRA-20% was higher than the control sample. At 28 days, the flexural strength of P-FRA-10% and P-FRA-15% were 1.15 and 1.08 times greater than those of P-FRA-0%. Both the compressive and flexural strengths of the P-FRA-10% were the highest. This means that the optimal addition ratio is 10% for adding FRA as a cement additive, which is the same as rice husk ash results (Bie *et al.* 2015). The P-FRA-10% can increase both compressive and flexural strengths by approximately 15%.

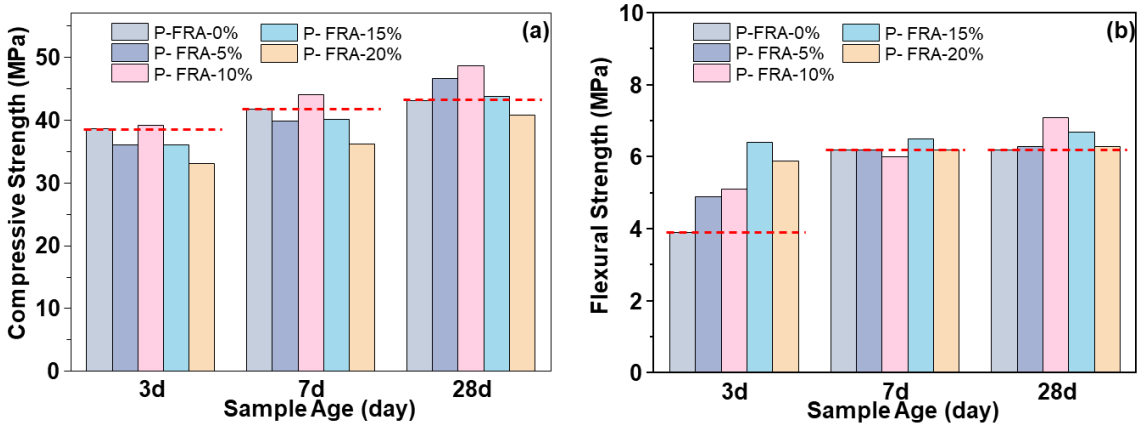

Fig. 3. Column charts of strength tests: (a) compressive strength, (b) flexural strength

Figures 4 and 5 depict the microstructures observed after a 28-day period with and without aggregate when the cement was replaced by 0%, 5%, 10%, 15%, and 20% FRA, respectively. The specimens exhibited a densification of the microstructure following a 28-day period of hydration. Interfacial irregularities can be seen between the aggregate and the binder paste in the specimens (Fig. 4). As shown in Fig. 4b-e, several products resembling cotton formed surrounding the aggregates. These products can absorb the energy generated by the expansion reaction, and the alkali silicate reaction has been prevented. As shown in Fig. 4c and f, there were more cotton-like structures around the aggregate making a dense structure to resist deformation. There were more ettringite needles and cotton-like products after introduced FRA as cement additive (Fig. 5), especially when the is FRA was corresponding to 10% of the cement weight, as shown in Fig. 5c. It can be said that introducing FRA will enhance the reactive silica content, thereby facilitating the formation of calcium silicate hydrate (C-S-H) and optimizing the pore structure. Consequently, cement mortar compressive strength will increase with its cotton-like and ettringite needles characteristics. As a result, the series P-FRA-10% had the greatest compressive strength values which was 40.6 MPa, increased by approximately 15%.

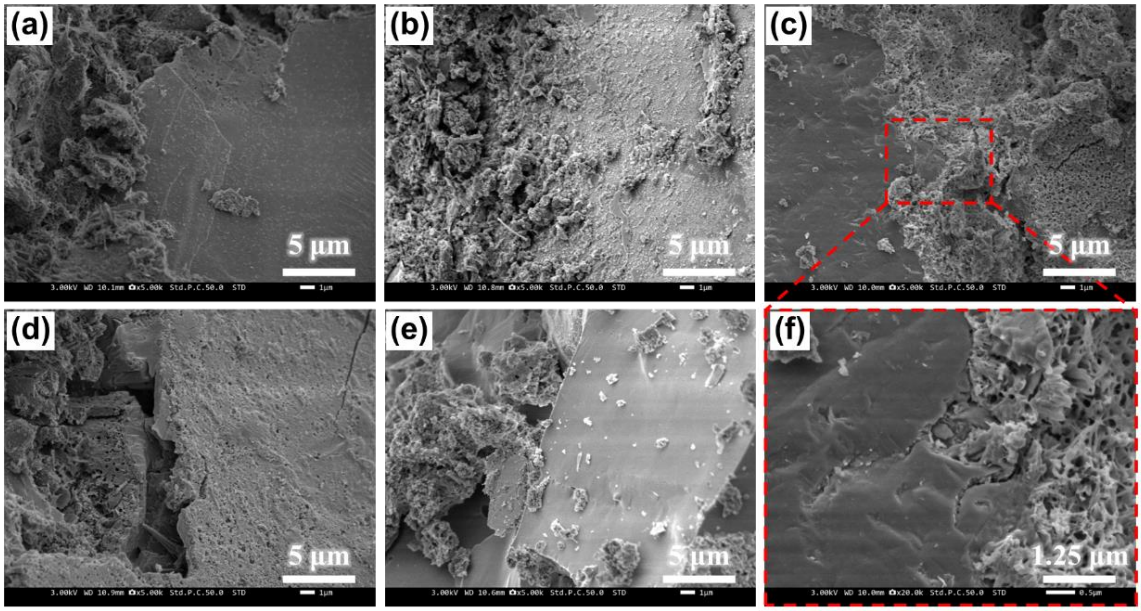

Fig. 4. SEM micrographs after 28 days with aggregate. P-FRA-0% (a), P-FRA-5% (b), P-FRA-10% (c), P-FRA-15% (d), P-FRA-20% (e) under a magnification of 5000, and P-FRA-10% (f) under a magnification of 20000

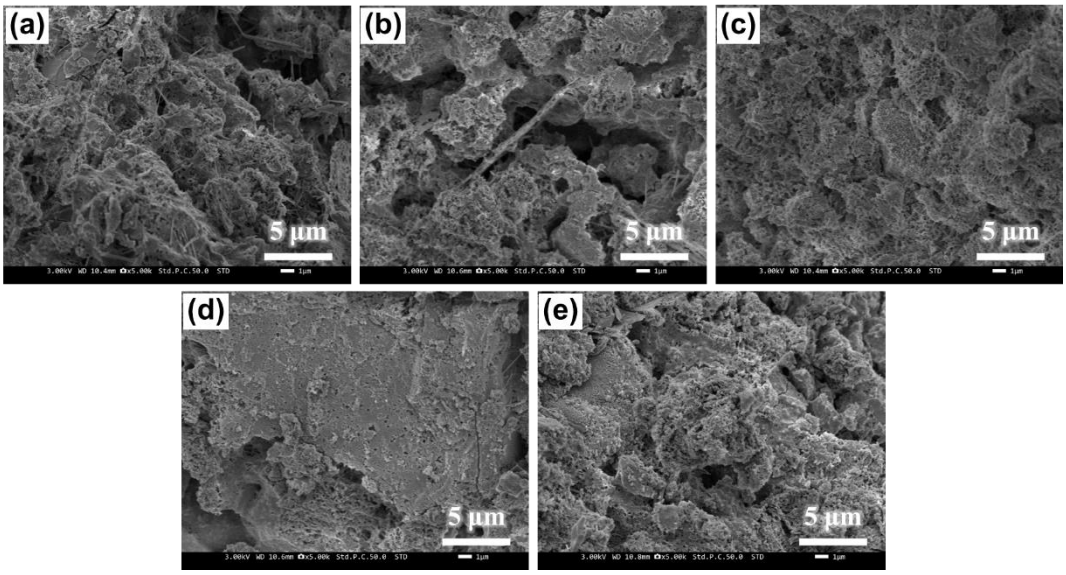

Fig. 5. SEM micrographs after 28 days without aggregate. P-FRA-0% (a), P-FRA-5% (b), P-FRA-10% (c), P-FRA-15% (d), P-FRA-20% (e), under a magnification of 5000

Strength of Magnesium Oxysulfate Cement Mortar

The compressive strength data of FRA blended in magnesium oxysulfate mortar are shown in Fig. 6. In terms of compressive strength, the modified magnesium oxysulfate cement initially increased and then decreased with the addition of FRA. When the ash content reached 10 wt%, the compressive strength peaked at 44.3 MPa, an improvement of 12.7% compared to the reference specimen without the aggregate. This indicates that the addition of FRA enhances the compressive strength of the modified magnesium oxysulfate cement, likely due to the ash filling the voids in the cement matrix, thereby increasing its density.

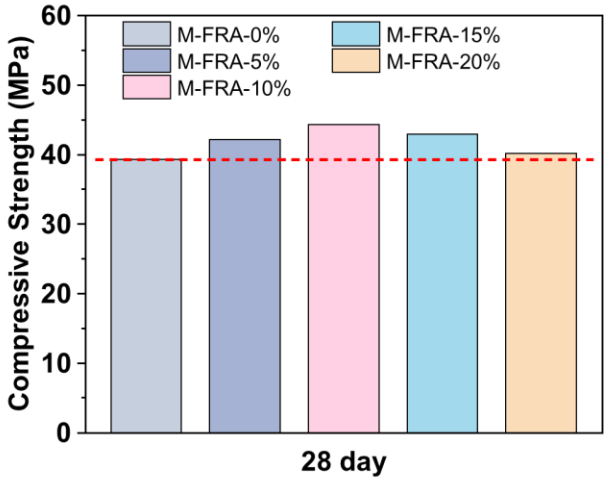

Fig. 6. Column charts of compressive strength tests for magnesium oxysulfate mortar

Figure 7 shows the phase composition of modified magnesium oxysulfate cement with varying amounts of FRA. When the ash content was 0, the primary phases were 5·1·7 and $Mg(OH)_2$.

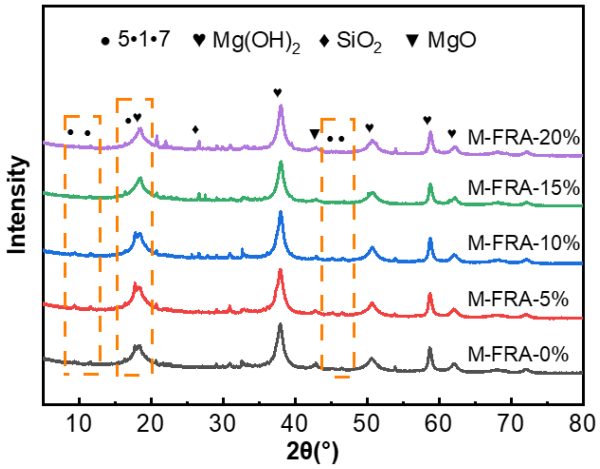

Fig. 7. XRD results of modified magnesium oxysulfate cement mortar

With the addition of 5 and 10 wt% ash, the phase composition changed significantly, with the diffraction peak of the 5·1·7 phase gradually increasing. Compared with the M-FRA-0%, no new phases were generated, indicating that the ash did not chemically react with the cement to form new substances. As the ash content further increased, the diffraction peak of the 5·1·7 phase disappeared, suggesting that a small amount of ash promotes the formation of the 5·1·7 phase, while excessive ash inhibits its formation.

Figure 8 presents the microstructure of modified magnesium oxysulfate cement with and without FRA. The sample containing 10 wt.% FRA exhibited a notable formation of short, needle-like crystals anchored to block crystals, in contrast to the reference sample without FRA. This observation suggests that incorporating FRA enhances the formation of the 5·1·7 phase, aligning with the findings from the XRD analysis and compressive strength tests.

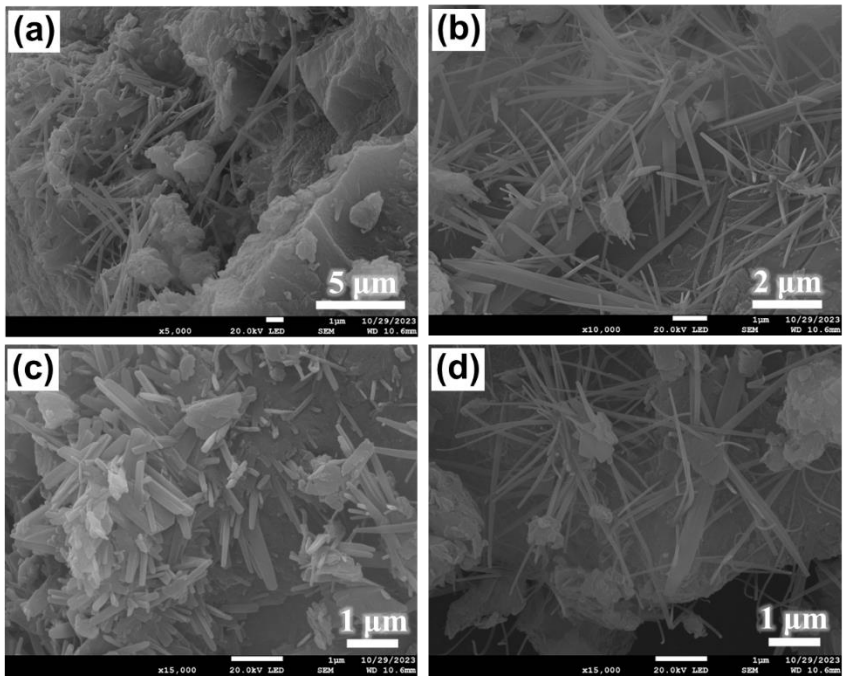

Fig. 8. SEM micrographs after 28 days of series M-FRA-0% (a), M-FRA-5% (b), M-FRA-10% (c), M-FRA-15% (d), M-FRA-20% (e) under a magnification of 5000

CONCLUSIONS

This study investigated the potential of incorporating furfural residue ash (FRA) as an additive in both Portland cement and magnesium oxysulfate cement. The findings, based on strength tests, X-ray diffraction (XRD), and scanning electron microscopy (SEM) analyses, are as follows:

1. For Portland cement, the addition of 10 wt% FRA promoted the formation of cotton-like structures and needle-shaped ettringite, thereby enhancing the cement's density and mechanical properties. Compared to the control sample, both the compressive and flexural strengths of the cement increased by approximately 15%.
2. For magnesium oxysulfate cement, the addition of 10 wt.% FRA effectively promoted the formation of the 5·1·7 phase, which plays a key role in enhancing the compressive strength of this type of cement. This phase contributed to a significant improvement in the cement's structural density and overall strength. Compared to the control sample, the compressive strength increased by 12.7%, reaching 44.3 MPa.
3. FRA exhibited significant performance enhancements when used as an additive in both Portland cement and magnesium oxysulfate cement. This finding also opens possibilities for its application as an additive in other types of cement, paving the way for the resource utilization of this type of solid waste.

ACKNOWLEDGMENTS

This study was supported by the Key Research and Development Project of Hainan Province (ZDYF2022SHFZ315) and the Natural Science Foundation of Liaoning Province (2022-NLTS18-04). We also extend our gratitude to the authors of the cited references for providing essential data and information. This research did not receive any specific grant from funding agencies in the public, commercial, or not-for-profit sectors.

REFERENCES CITED

Adesanya, D. A., and Raheem, A. A. (2009). "A study of the workability and compressive strength characteristics of corn cob ash blended cement concrete," *Construction and Building Materials* 23(1), 311-317. DOI: 10.1016/j.conbuildmat.2007.12.004

Bie, R., Song, X., Liu, Q., Ji, X., and Chen, P. (2015). "Studies on effects of burning conditions and rice husk ash (RHA) blending amount on the mechanical behavior of cement," *Cement and Concrete Composites* 55, 162-168. DOI: 10.1016/j.cemconcomp.2014.09.008

Chou, L. H., Lu, C. K., Chang, J. R., and Lee, M. T. (2007). "Use of waste rubber as concrete additive," *Waste Management and Research* 25(1), 68-76. DOI: 10.1177/0734242X07067448

Endashaw, D. K,. (2022). "Influence of corn cob ash as a filler material in asphalt concrete mixes," *International Journal of Pavement Research and Technology* 16, 1217-1225. DOI: 10.1007/s42947-022-00191-w.

Favier, A., De Wolf, C., Scrivener, K., and Habert, G. (2018). "A sustainable future for the European Cement and Concrete Industry: Technology assessment for full decarbonisation of the industry by 2050," *ETH Zurich*. DOI: 10.3929/ethz-b-000301843

GB/T 17671-1999 (1999). "Method of testing cements – Determination of strength," Standardization Administration, Beijing, China.

Guo, X., Zhang, X., Wang, Y., Tian, X., and Qiao, Y. (2022). "Converting furfural residue wastes to carbon materials for high performance supercapacitor," *Green Energy and Environment* 7(6), 1270-1280. DOI: 10.1016/j.gee.2021.01.021

Guo, Z., Wang, S., and Bai, D. (2023). "Engineering thermochemistry: The science critical for the paradigm shift toward carbon neutrality," *Resources Chemicals and Materials* 2(4), 331-334. DOI: 10.1016/j.recm.2023.11.001

Han, Z., Jia, X., Song, X., An, P., Fu, L., Yue, J., Yu, J., Liu, X., Zhang, Z., Jin, Y., He, M., Bai, D., and Xu, G. (2023). "Engineering thermochemistry to cope with challenges in carbon neutrality," *Journal of Cleaner Production* 416, article ID 137943. DOI: 10.1016/j.jclepro.2023.137943

He, Z., Zhu, X., Wang, J., Mu, M., and Wang, Y. (2019). "Comparison of CO_2 emissions from OPC and recycled cement production," *Construction and Building Materials* 211, 965-973. DOI: 10.1016/j.conbuildmat.2019.03.289

IEA (2024), CO_2 Emissions in 2023, IEA, Paris. https://www.iea.org/reports/co2-emissions-in-2023, Licence: CC BY 4.0.

Inkoua, S., Li, C., Fan, H., Kontchouo, F. M. B., Sun, Y., Zhang, S., and Hu, X. (2022). "Pyrolysis of furfural residues: Property and applications of the biochar," *Journal of Environmental Management* 316, article ID 115324. DOI: 10.1016/j.jenvman.2022.115324

JC/T 724-2005. (2005). "Method of testing cements – Determination of strength," Standardization Administration, Beijing, China.

Jiang, W., Xing, X., Li, S., Zhang, X., and Wang, W. (2019). "Synthesis, characterization and machine learning based performance prediction of straw activated carbon," *Journal of Cleaner Production* 212, 1210-1223. DOI: 10.1016/j.jclepro.2018.12.093

Liu, Y., Wu, S., Zhang, H., and Xiao, R. (2020). "Preparation of carbonyl precursors for long-chain oxygenated fuels from cellulose ethanolysis catalyzed by metal oxides," *Fuel Processing Technology* 206, article ID 106468. DOI: 10.1016/j.fuproc.2020.106468

Mao, X., Kang, Q., Liu, Y., Siyal, A., Ao, W., Ran, C., Fu, J., Deng, Z., Song, Y., and Dai, J. (2019). "Microwave-assisted pyrolysis of furfural residue in a continuously operated auger reactor: Biochar characterization and analysis," *Energy* 168, 573-584. DOI: 10.1016/j.energy.2018.11.055

Oluremi, J. R., Raheem, A. A., Balogun, R. O., and Moshood, A. A. (2023). "Early strength development assessment of concrete produced from cement replaced with nano silica activated corn cob ash," *Materials Today: Proceedings* 86, 36-40. DOI: 10.1016/j.matpr.2023.02.191

Oriola, K. O., Raheem, A. A., and Ogundele, A. B. (2023). "Investigation of compressive strength and thermal properties of corn cob ash cement concrete," *Materials Today: Proceedings* 86, 128-133. DOI: 10.1016/j.matpr.2023.04.520

Rachamontree, P., Douzou, T., Cheenkachorn, K., Sriariyanun, M., and Rattanaporn, K. (2020). "Furfural: A sustainable platform chemical and fuel," *Applied Science and Engineering Progress* 13(1), 3-10, article ID 239991. DOI:

index.php/ijast/article/view/239991

Ranjbari, M., Esfandabadi, Z. S., Quatraro, F., Vatanparast, H., Lam, S. S., Aghbashlo, M., and Tabatabaei, M. (2022). "Biomass and organic waste potentials towards implementing circular bioeconomy platforms: A systematic bibliometric analysis," *Fuel* 318, article ID 123585. DOI: 10.1016/j.fuel.2022.123585

Samad, S., Shah, A., and Limbachiya, M. C. (2017). "Strength development characteristics of concrete produced with blended cement using ground granulated blast furnace slag (GGBS) under various curing conditions," *Sādhanā* 42, 1203-1213. DOI: 10.1007/s12046-017-0667-z

Sirico, A., Bernardi, P., Sciancalepore, C., Vecchi, F., Malcevschi, A., Belletti, B., and Milanese, D. (2021). "Biochar from wood waste as additive for structural concrete," *Construction and Building Materials* 303, article ID 124500. DOI: 10.1016/j.conbuildmat.2021.124500

Smit, A. T., and Huijgen, W. J. J. (2017). "The promotional effect of water-soluble extractives on the enzymatic cellulose hydrolysis of pretreated wheat straw," *Bioresource Technology* 243, 994-999. DOI: 10.1016/j.biortech.2017.07.072

Solahuddin, B. A., and Yahaya, F. M. (2022). "Properties of concrete containing shredded waste paper as an additive," *Materials Today: Proceedings* 51, 1350-1354. DOI: 10.1016/j.matpr.2021.11.390

Song, X., Jia, X., An, P., Han, Z., and Xu, G. (2024). "Development of science and technology in thermochemical reaction engineering," *Chemical Industry and Engineering Progress* 43(7), 3513. DOI: 10.16085/j.issn.1000-6613.2024-0315

Stonis, R., Pundiene, I., Antonoviè, V., Kligis, M., and Spudulis, E. (2013). "Study of the effect of replacing microsilica in heat-resistant concrete with additive based on metakaolin," *Refractories and Industrial Ceramics* 54(3), 232-237. DOI: 10.1007/s11148-013-9580-0

Wang, Y., Xu, Z. Y., Song, X., Yang, B., and Zhang, D. (2017). "The preparation of low-cost adsorbent for heavy metal based on furfural residue," *Materials and Manufacturing Processes* 32(1), 87-92. DOI: 10.1080/10426914.2016.1198017

Xu, G., Bai, D., Xu, C., and He, M. (2023). "Challenges and opportunities for engineering thermochemistry in carbon-neutralization technologies," *National Science Review* 10(9), article nwac217. DOI: 10.1093/nsr/nwac217

Yemiş, O., and Mazza, G. (2011). "Acid-catalyzed conversion of xylose, xylan and straw into furfural by microwave-assisted reaction," *Bioresource Technology* 102(15), 7371-7378. DOI: 10.1016/j.biortech.2011.04.050

Article submitted: August 28, 2024; Peer review completed: September 15, 2024;
Revised version received and accepted: September 23, 2024; Published: October 8, 2024.
DOI: 10.15376/biores.19.4.8947-8958